Interface Energetics and Level Alignment at Covalent Metal-Molecule Junctions: π-Conjugated Thiols on Gold

Georg Heimel,[1] Lorenz Romaner,[1,2] Jean-Luc Brédas,[1] and Egbert Zojer[1,2]

[1]*School of Chemistry and Biochemistry and Center for Organic Photonics and Electronics, Georgia Institute of Technology, Atlanta, Georgia 30332-0400, USA*
[2]*Institute of Solid State Physics, Graz University of Technology, Petersgasse 16, A-8010 Graz, Austria*
(Received 12 December 2005; published 17 May 2006)

The energetics at the interfaces between metal and monolayers of covalently bound organic molecules is studied theoretically. Despite the molecules under consideration displaying very different frontier orbital energies, the highest occupied molecular levels are found to be pinned at a constant energy offset with respect to the metal Fermi level. In contrast, the molecular properties strongly impact the metal work function. These interfacial phenomena are rationalized in terms of charge fluctuations and electrostatics at the atomic length scale as determined by *first-principles* calculations.

The key role of the interface between metal electrode and organic semiconductor is well acknowledged in the context of organic (opto)electronic devices [1]. Self-assembled monolayers (SAMs) [2] of dipolar organic molecules provide a pathway to tune the barriers for charge-carrier injection into the active organic layer at the *molecular* scale by modifying the effective work function, Φ, of the electrodes and thus adjusting the alignment of the metal Fermi energy E_F with the conduction states in the organic semiconductor [3]. In addition, SAMs of π-conjugated thiols have been extensively studied for single-molecule electronics [4]. Here, the metal-molecule contact, at the *atomic* length scale, defines the alignment of the frontier orbitals of the active molecular entity with E_F [5,6]. In particular, the energy separation ΔE between E_F and the closest molecular level (typically the highest occupied molecular orbital, HOMO) is one of the main parameters governing the overall device characteristics [6].

In this work, we theoretically explore the possibility of tuning the interface energetics in molecular electronic devices by modifying (via chemical substitution) the ionization potential (*IP*) of a prototype π-conjugated thiol assembled on gold. Most interestingly, while the modification, $\Delta\Phi$, of the Au(111) work function *strongly* depends on the molecular *IP*s, the level alignment ΔE is *not* affected. Understanding the connection between these two quantities provides a deeper insight into the parameters governing the general properties of metal-organic interfaces.

The 4′-substituted 4-mercaptobiphenyls were chosen as model compounds because they are experimentally well characterized for a large number of substituents *X* [7,8]. In particular, we chose $X = NH_2$, CN, and SH. The strong donor (NH_2) shifts the frontier molecular orbitals (MOs) up in energy while the strong acceptor (CN) shifts them down; the symmetric substitution (SH) serves for reference purposes. The molecules were arranged in a $c(\sqrt{3} \times 3)$

herringbone adlayer on the Au(111) substrate [Fig. 1(b)] [9]. We assume the same arrangement for all three molecules for reasons of comparability, although it cannot be excluded that electrostatic repulsion [8] somewhat limits the achievable packing density for the two dipolar compounds $X = NH_2$ and CN.

The surface was modeled using the *repeated-slab* approach, where 5 layers of gold were used to represent the Au(111) surface in the lateral unit cell mentioned above (Fig. 1). The vacuum gap between the topmost molecular atom and the next slab was >22 Å. Isolated molecules were calculated in a 3D periodically repeated box of $20 \times 20 \times 30$ Å. We performed density functional theory (DFT) calculations with the PW91 exchange-correlation functional, using a plane-wave basis set (cutoff 20 Ry) for the valence electrons and the projector augmented-wave method [10] to describe the valence-core interactions. An $8 \times 5 \times 1$ Monkhorst-Pack grid of *k* points was employed. The atomic positions in the molecules and the top two gold layers were fully relaxed until the remaining forces were <0.01 eV/Å, resulting in the adsorption geometry depicted in Fig. 1. All calculations were performed with the
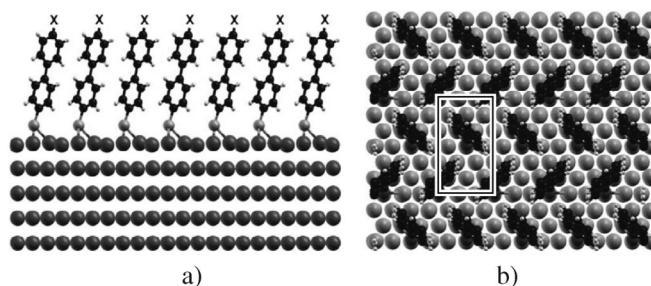

FIG. 1. Side (a) and top (b) view of the SAM structure of 4′-*X*-4-mercaptobiphenyl on Au(111) where $X = NH_2$, SH, and CN. The $c(\sqrt{3} \times 3)$ surface unit cell is indicated by the contour in (b).

VASP code [11]. The HOMO energies in the molecular layers were taken to be the highest-energy peak in the respective density of states [12]. The robustness of the results with respect to all computational parameters was thoroughly tested.

The main results are summarized in Table I. Rather surprisingly, it is found that, in spite of very different molecular *IP*s, the molecular HOMOs for all three substitutions come to lie at virtually identical ΔEs below E_F. In strong contrast, the adsorbate-induced changes in the metal work function markedly depend on the substitution: strong work function increase for the acceptor group ($X =$ CN), intermediate decrease for the symmetric substitution ($X =$ SH), and strong decrease for the donor group ($X =$ NH$_2$).

In order to conceptually understand these remarkable findings, the SAM formation will be discussed as a 3-step process: (i) the isolated molecules and the clean Au(111) surface are separated; (ii) a molecular monolayer is formed in the same geometry as that eventually adopted in the SAM; (iii) this layer is deposited onto the gold surface (thiols are assumed to adsorb with hydrogen removal). Computationally, these three steps are modeled by performing calculations on: (a) a clean gold surface with the atomic positions in its top two layers fully relaxed; (b) the geometry-relaxed isolated molecules; (c) the final geometry-relaxed system made of the SAM adsorbed on the surface; (d) the clean gold surface with its atomic positions taken from (c); (e) the single molecular layer with the geometry of (c) where each sulfur is saturated with a hydrogen whose position is optimized (no gold is present in this step), and (f) this layer of hydrogens alone [13].

Starting with (a), we find $\Phi_{\mathrm{Au(111)}} = 5.20$ eV, defined as the difference between the electrostatic potential in the vacuum region (V_{vac}) and E_F [Fig. 2(a)]. The molecular *IP*s (defined as the energy difference between the HOMO and V_{vac} [12]) for $X =$ NH$_2$, SH, and CN are listed in Table I [see also Fig. 2(a)]. As expected, that of the donor substituted molecule ($X =$ NH$_2$) is lowest and that of the acceptor substituted molecule ($X =$ CN) is highest.

Arranging the molecules in the close-packed layer corresponding to their final adsorption geometry aligns their dipole moments (when present). While the electrostatic

potential around any single isolated molecule converges to a single vacuum level V_{vac} at a sufficiently large distance in any direction (and thus permits the unique definition of a single *IP*), the 2D infinite dipole layer formed in part (e), divides space into two regions with different vacuum levels $V_{\mathrm{vac}}^{\mathrm{left}}$ and $V_{\mathrm{vac}}^{\mathrm{right}}$ [Fig. 2(b)]. This causes a step $\Delta V_{\mathrm{vac}} = V_{\mathrm{vac}}^{\mathrm{right}} - V_{\mathrm{vac}}^{\mathrm{left}}$ in the electrostatic potential across this layer (Table I). Consequently, the *IP* of the molecular layer now depends on which side an electron is extracted from [Fig. 2(b)]; there is a left (thiol) and a right (substitution X) *IP*, IP^{left}, and IP^{right} (Table I). For all three molecules, the IP^{left} values are practically identical [Table I and Fig. 2(b)] [12]. In contrast, the IP^{right} values strongly depend on the substituent X, and the trend in the molecular *IP*s is significantly enhanced. Thus, the donor-acceptor groups X affect only "their end" of the molecular layer, while the π-conjugated core and the thiol side of the layer (facing the gold surface) are hardly affected [Fig. 2(b)].

Conceptually, the adsorption of the molecular layer onto the Au(111) surface can be described as follows: The thiol hydrogens are removed from the molecular layer [i.e., the charge density, ρ_H, associated with the hydrogen layer [part (f)] is subtracted from that of the molecular layer, ρ_{mol}, part (e)]; instead of this layer of hydrogens, the Au(111) surface is placed next to the molecular layer [i.e., its charge density, ρ_{Au}, is added; part (d)]. The charge reorganization upon S-Au bond formation, ρ_{diff}, is then given by the difference between these superimposed charge densities and the actual equilibrated density, ρ, of the final combined Au(111)-SAM system [part (c)]:

$$\rho_{\mathrm{diff}} = \rho - (\rho_{\mathrm{mol}} - \rho_H + \rho_{\mathrm{Au(111)}}) \qquad (1)$$

It thus represents the difference between bonding of the molecular layer to gold vs the bonding to the thiol hydrogens [Fig. 3(a)]. The following important conclusions can be drawn from Fig. 3(a): Integrating over ρ_{diff} (within the uncertainty of where the metal actually ends and the molecule begins) yields no net charge transfer from metal to molecule or *vice versa* in spite of the significant offsets (Table I) between the molecular *IP*s and $\Phi_{\mathrm{Au(111)}}$ [12]. Rather, a series of dipoles is induced upon adsorption, which suggests looking at charge transfer in a more local way (e.g., between Au and S, ρ_{diff} clearly indicates the

TABLE I. HOMO energy relative to E_F (ΔE), work function modification ($\Delta\Phi$), molecular ionization potentials (*IP*), left and right ionization potentials (IP^{left} and IP^{right}) of the hydrogen terminated layers of molecules, steps in the vacuum level across the molecular layer (ΔV_{vac}), BD, ionization potential of the adsorbed SAM ($IP^{\mathrm{right}}_{\mathrm{SAM}}$), and energy correction to the HOMO level (E_{corr}). All values are given in units of eV (per elementary charge); X denotes the substituent.

X	ΔE	$\Delta\Phi$	IP	IP^{left}	IP^{right}	ΔV_{vac}	BD	$IP^{\mathrm{right}}_{\mathrm{SAM}}$	E_{corr}
NH$_2$	-0.96	-2.69	4.81	5.12	3.62	-1.49	-1.19	3.47	0.15
SH	-0.95	-1.02	5.16	5.08	5.27	0.19[a]	-1.19	5.13	0.13
CN	-0.99	2.66	5.69	5.17	9.01	3.84	-1.17	8.84	0.16

[a]For the symmetric substitution, ΔV_{vac} arises from the fact that the (slightly asymmetric) atomic positions of the final relaxed structure of the adsorbed SAM were used for the hydrogen terminated molecular layer.
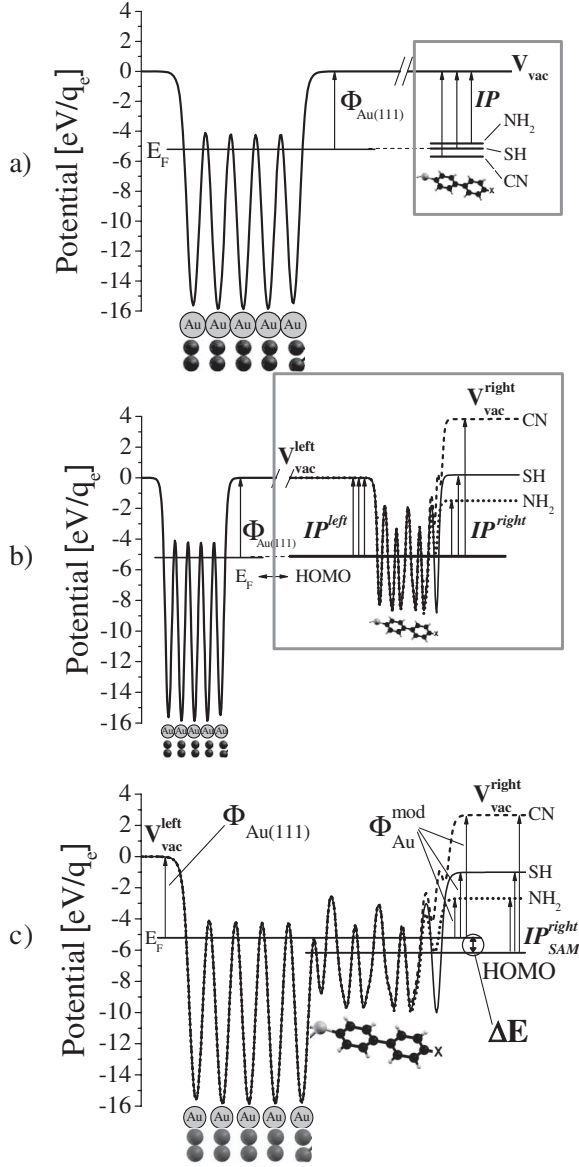
FIG. 2.   (a) Plane-averaged electrostatic potential (eV per elementary charge q_e) of a 5-layer Au(111) slab (left). Also indicated is the metal Fermi energy E_F, its work function $\Phi_{Au(111)}$, the vacuum level V_{vac}, and the molecular HOMO levels (horizontal lines, right) as well as the molecular ionization potentials (IP). (b) Plane-averaged electrostatic potential, left and right vacuum levels (V_{vac}^{left}, V_{vac}^{right}) and ionization potentials (IP^{left}, IP^{right}) of the hydrogen terminated molecular layers (right) compared to the isolated gold slab (left). (c) Potential of the SAMs adsorbed onto Au(111). The HOMO is located at ΔE below E_F, $\Phi_{Au(111)}$ is changed to Φ_{Au}^{mod}, and IP^{right} to IP_{SAM}^{right}. The gray boxes indicate that the isolated molecules and the hydrogen terminated molecular layers have been calculated separately, in the absence of any gold.

formation of a bond). The charge rearrangement upon SAM formation rapidly decays in both the metal (within the first two layers) and the SAM (within the first aromatic ring). Moreover, ρ_{diff} is virtually identical for all systems

(note that in Fig. 3(a) data are shown for all three compounds), underlining that the very different offsets between the molecular IPs and $\Phi_{Au(111)}$ are inconsequential for the charge rearrangement at the S-Au interface.

Since ρ_{diff} is essentially a series of dipole layers, it leads to an additional potential step across the S-Au bonding region. Numerically integrating the (one-dimensional) Poisson equation $\nabla^2 V = -\rho_{diff}/\varepsilon_0$ yields the microscopic structure [Fig. 3(b)] and magnitude (Table I) of this interfacial *bond dipole*, BD [3,14]. The main effect of BD (calculated to be ca. -1.2 eV [14,15]) is to rigidly shift the potential well of the whole molecular layer, in particular V_{vac}^{right}, relative to the potential inside the metal, its electronic states, and E_F [Fig. 2(c)]; the molecular levels are shifted accordingly. As a secondary effect, the modification of the potential at the sulfur atoms and, to a lesser extent, on the first aromatic ring [Fig. 3(b)] results in a small renormalization of the MO energies. The magnitude, E_{corr}, of this perturbation for the HOMO is determined by the difference between IP^{right} and the IP of the adsorbed SAM, IP_{SAM}^{right} [Fig. 2(c)]. We find a slight destabilization of the HOMO with respect to V_{vac}^{right} (Table I).

The values obtained for ΔE and $\Delta\Phi$ (Table I) can now be rationalized on the basis of the more instructive microscopic description developed above: As was stressed before, what is relevant for the level alignment are *not* the
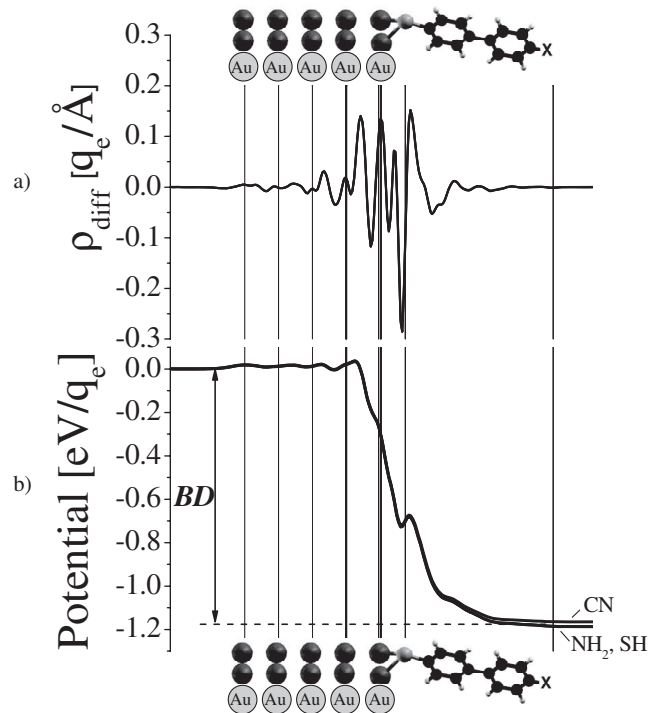

FIG. 3.   Plane-integrated charge density difference ρ_{diff} (a) in units of elementary charge $q_e/\text{Å}$ and the electrostatic potential drop BD (b) across the SAM/metal interface resulting from the difference between the S-H and S-Au bonding in eV per elementary charge q_e. The vertical lines mark the positions of the gold, sulfur, and substitution (X) atoms.

molecular IPs (lying somewhere between IP^{left} and IP^{right}), but rather the offsets between IP^{left} and $\Phi_{\text{Au(111)}}$ [12]. Starting from this energy difference, the HOMO of the molecular layer is then shifted by BD and corrected by E_{corr} to yield ΔE (its energetic position relative to E_F):

$$\Delta E = \Phi_{\text{Au(111)}^-} IP^{\text{left}} + \text{BD} + E_{\text{corr}} \qquad (2)$$

Because the IP^{left} values are virtually identical for all three compounds (as are the BD and E_{corr} values), also the ΔE values are practically the same (Table I). Thus, all HOMOs line up at the same energy below E_F [Fig. 2(c)] [12,15].

In contrast, the modification of the gold work function, which can be expressed as [3,14]:

$$\Delta\Phi = \Delta V_{\text{vac}} + \text{BD} \qquad (3)$$

is very different for the three investigated molecules (Table I). The numbers reported in this Letter should be regarded as upper limits for what can be observed in experiments, where the high coverage and order assumed for the calculations can be realized locally at the best [8,9]. Note that the choice of the symmetric substitution $X = \text{SH}$ conveniently provides direct access to the BD at the S-Au interface, since here $\Delta\Phi \approx \text{BD}$ (the difference of ca. 0.2 eV is due to the geometry distortion of the isolated molecule upon adsorption into the SAM). The values for ΔE [$\Delta\Phi$] obtained via Eq. (2) [Eq. (3)] are within max. 0.02 eV of those extracted from the self-consistent calculations on the full systems [part (c)].

To summarize, we theoretically studied representative π-conjugated organic molecules assembled on, and covalently bound to a metal electrode. We focused on the mechanism of level alignment and work function modification. Our work demonstrates that, for such systems, an offset between the molecular IPs and $\Phi_{\text{Au(111)}}$ alone does *not* give rise to any net long-range charge transfer and, thus, does not impact the alignment of the HOMOs with the metal E_F. Rather, the local electrostatic potential at the binding site of the (closely packed layer of) molecules must be considered together with the localized charge fluctuations at the metal-molecule interface induced by the covalent bond formation. Consequently, the molecular HOMOs line up at the same energy below E_F *regardless* of chemical substitutions outside the immediate interfacial region. The work function of the SAM covered gold surface, however, can be tuned over a wide range. By shedding new light onto the general properties of molecule/metal interfaces at the atomic level, our findings suggest that different strategies need to be applied depending on whether the SAM is to act as the active transporting entity or as the injection promoting entity in (macroscopic) organic electronic devices.

[1] H. Ishii, K. Sugiyama, E. Ito, and K. Seki, Adv. Mater. **11**, 605 (1999).
[2] F. Schreiber, Prog. Surf. Sci. **65**, 151 (2000).
[3] I. H. Campbell, S. Rubin, T. A. Zawodzinski, J. D. Kress, R. L. Martin, D. L. Smith, N. N. Barashkov, and J. P. Ferraris, Phys. Rev. B **54**, R14 321 (1996).
[4] J. Chen, M. A. Reed, A. M. Rawlett, and J. M. Tour, Science **286**, 1550 (1999).
[5] T. Vondrak, H. Wang, P. Winget, C. J. Cramer, and X. Y. Zhu, J. Am. Chem. Soc. **122**, 4700 (2000).
[6] Y. Q. Xue, S. Datta, and M. A. Ratner, J. Chem. Phys. **115**, 4292 (2001).
[7] J. F. Kang, A. Ulman, S. Liao, R. Jordan, G. H. Yang, and G. Y. Liu, Langmuir **17**, 95 (2001).
[8] J. F. Kang, S. Liao, R. Jordan, and A. Ulman, J. Am. Chem. Soc. **120**, 9662 (1998).
[9] W. Azzam, C. Fuxen, A. Birkner, H. T. Rong, M. Buck, and C. Wöll, Langmuir **19**, 4958 (2003).
[10] G. Kresse and D. Joubert, Phys. Rev. B **59**, 1758 (1999).
[11] G. Kresse and J. Furthmüller, Phys. Rev. B **54**, 11 169 (1996).
[12] While trends upon substitution are fully captured, Kohn-Sham orbital energies of state-of-the-art DFT notoriously underestimate the IPs of small molecules. This effect is expected to be less severe for the ΔE values, where only the relative energies of states associated with parts of a larger metallic system are concerned, which can equilibrate electronically.
[13] Because spin-polarized and -unpolarized calculations yield the same results to within <5 meV/q_e, only spin-unpolarized (restricted) calculations are presented in this study.
[14] V. De Renzi, R. Rousseau, D. Marchetto, R. Biagi, S. Scandolo, and U. del Pennino, Phys. Rev. Lett. **95**, 046804 (2005).
[15] Work function changes and dipole layers are known to be adequately described at the DFT level employed in this work. Because of a potential underestimation of the molecular IPs, the BD and the (negligible) amount of charge transfer give an upper boundary to what can be expected for real systems.